Anomalous hydrogen adsorption sites found for the $c(2\times2)-3H$ phases formed on the Re(1010) and Ru(1010) surfaces

Cite as: J. Chem. Phys. **108**, 8671 (1998); https://doi.org/10.1063/1.476296
Submitted: 05 January 1998 . Accepted: 17 February 1998 . Published Online: 13 May 1998

R. Döll, L. Hammer, K. Heinz, K. Bedürftig, U. Muschiol, K. Christmann, A. P. Seitsonen, H. Bludau, and H. Over

Anomalous hydrogen adsorption sites found for the $c(2\times2)$-3H phases formed on the Re(1010) and Ru(1010) surfaces

R. Döll, L. Hammer, and K. Heinz
Lehrstuhl für Festkörperphysik, Universität Erlangen-Nürnberg, Staudtstr. 7, D-91058 Erlangen, Germany

K. Bedürftig, U. Muschiol, and K. Christmann
Institut für Physikalische und Theoretische Chemie, Freie Universität Berlin, Takustr. 3, D-14195 Berlin, Germany

A. P. Seitsonen, H. Bludau, and H. Over[a)]
Fritz-Haber-Institut der Max-Planck-Gesellschaft, Faradayweg 4-6, D-14195 Berlin, Germany

(Received 5 January 1998; accepted 17 February 1998)

Hydrogen adsorption on the $(10\bar{1}0)$ surfaces of Ru and Re leads to the formation of $c(2\times2)$-3H phases. As determined by quantitative low-energy electron diffraction (LEED) and density functional theory calculations, hydrogen atoms, as expected, occupy threefold coordinated hcp sites along the densely packed rows and the unexpected short-bridge sites along the ridges in both $c(2\times2)$ phases. The Ru and Re substrates reconstruct only weakly and in a very similar fashion under hydrogen chemisorption. Most notably, there is a buckling in the third substrate layer of about 0.06 Å. Probably (though not outside the limits of error), there are also slightly lateral displacements (0.02 Å) of top-layer substrate atoms which are bridge-coordinated to hydrogen. The metal–hydrogen bond lengths determined for both surfaces correspond to hydrogen radii in the expected range of 0.4–0.7 Å. © *1998 American Institute of Physics.* [S0021-9606(98)01320-8]

I. INTRODUCTION

In the past, numerous studies were devoted to the interaction of hydrogen with metal single-crystal surfaces, whereby, less frequently, adsorption geometries were also determined (for reviews, see Refs. 1–5). Various quantitative structure determinations using low-energy electron diffraction (LEED) and helium or neon diffraction (see, e.g., Refs. 5–7) disclosed that hydrogen atoms frequently prefer high-symmetry and high-coordinated adsorption sites. For hexagonal or nearly close-packed surfaces, such as fcc(111), hcp(0001), and bcc(110), or for close-packed microfacets on more open surfaces, such as fcc(110), these are the threefold coordinated hollow sites. Up to now, only for bcc(100) surfaces twofold symmetric bridge sites were identified for the H-saturated 1×1 phases on W(100),[8–10] Mo(100),[10,11] and $Mo_x\,Re_{1-x}$(100).[12] In the submonolayer regime, the bridge-bonding hydrogen atoms induce a dimerlike reconstruction of W(100)[9,10] and Mo(100).[10,11]

Hydrogen adsorption is usually accompanied by a modification of the geometric arrangement of substrate atoms. This effect ranges from the mere alteration of layer spacings, i.e., of the substrate's multilayer relaxation, over relatively weak substrate reconstructions with small displacements of atoms to severe bond breaking reconstructions which may even include the removal of substrate atoms.[5,13] In the latter two cases, the LEED intensities of the fractional order beams are governed by the substrate reconstruction, and therefore, the intensities are much larger than those expected from hydrogen scattering alone.

In view of the tendency of hydrogen to occupy high-coordinated sites, it is interesting to investigate H adsorption on more open surfaces with their variety of differently coordinated adsorption sites. Such a surface is that of hcp(1010) which is displayed in Fig. 1 with its two possible terminations. On Re(1010) and Ru(1010) hydrogen atoms order into a $c(2\times2)$ structure at coverage $\theta_H=3/2$ which transforms into a (1×1) structure at saturation coverage ($\theta_H=2$).[14–16] The strong LEED intensity of the fractional-order beams of both $c(2\times2)$-3H phases already indicates that at least some H-induced local displacements of the substrate atoms must be involved. The similarity between the chemically rather different metals extends also to the thermal desorption states of hydrogen, indicating that the H metal bondings are of comparable strengths at Re(1010) and Ru(1010). From these considerations it was proposed that the local adsorption geometry of the $c(2\times2)$-3H phases on Re(1010) and Ru(1010) surfaces should be very much alike.[16] Recalling that hydrogen atoms prefer to reside in high-coordinated sites, a tentative structure model was suggested[16] which allows for vertical displacements of single substrate atoms in the top layer to account for the strong LEED intensities of fractional order beams. Yet, this model was based on qualitative arguments rather than on a quantitative structure determination. In the present paper we close this gap and report on quantitative LEED analyses of the $c(2\times2)$-3H phases on Re(1010) and Ru(1010) which are supplemented by some first-principle calculations. It turns out that the picture of hydrogen adsorption described above is incomplete and that hydrogen atoms occupy threefold and twofold coordinated sites.

a)Author to whom correspondence should be addressed. Electronic mail: over@fhi-berlin.mpg.de; Fax: ++49-30-84135106.

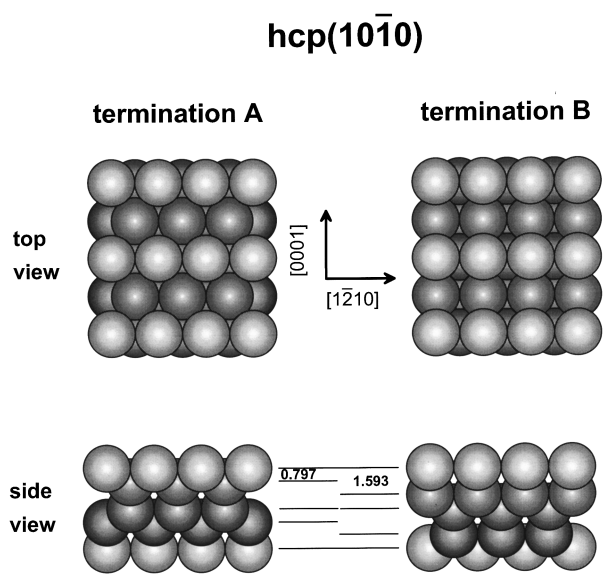

FIG. 1. Hard-sphere model of the hcp(10$\bar{1}$0) surface (numerical interlayer spacings are given for Re). For Ru the values are 0.78 and 1.56 Å, respectively.

II. EXPERIMENTAL AND COMPUTATIONAL DETAILS

Both the LEED experiments and the intensity analyses were carried out in different laboratories for the two surfaces. We therefore provide some details about the experiments and the data analyses separately for the two adsorption systems. The density functional theory (DFT) calculations were performed only for the H-Ru(1010) system. Both the Ru and Re sample consisted of small (area $\sim 1\ \mathrm{cm}^2$) single-crystal wavers of 5 N purity, x-ray oriented and cut to within 0.5° and mechanically polished.

A. Hydrogen adsorption on Re(10$\bar{1}$0)

The chamber contained four-grid backview LEED optics, a HREEL spectrometer, and a Kelvin probe for work function measurements. Rather high temperatures achieved by indirect heating had to be applied for the chemical cleaning of the Re sample through oxygen/hydrogen treatment. The clean surface was characterized by a sharp LEED pattern with a very low background as well as by Auger spectra which did not exhibit any indications of S, C, or O impurities. After preparation, the crystal was cooled to about 120 K and exposed to 15 L hydrogen. This was sufficient to produce the optimum coverage for the formation of the $c(2\times2)$-3H phase.[15,16] The fractional-order LEED spots were well visible exhibiting an energy averaged (50–400 eV) intensity level of about 6% with respect to integral-order beams. The LEED IV curves were collected at a sample temperature of about 120 K using a computer-controlled video technique.[17] Unfortunately, because of restrictions imposed by the sample holder, the exact adjustment of normal incidence of the primary beam was not possible. While the direction of incidence could be adjusted to fall within the (0001) plane, the incidence angle within that plane with respect to the surface normal could only be estimated ($\theta \approx 3.4°$). Moreover, upon varying the energy, it was not possible to keep this angle strictly constant because of residual magnetic and/or electric fields. As a consequence, the degeneracy of beams symmetrically equivalent at normal incidence is lifted, yielding a rather large cumulative width of the data base. For the clean surface the total energy range was 3900 eV by measuring 16 symmetrically inequivalent beams in the energy range 50–400 eV. For the $c(2\times2)$-3H phase 13 symmetrically inequivalent integral-order and nine half-order beams were analyzed corresponding to a total data base of 3280 eV. Of course, not knowing the precise angle of incidence θ and its variation with energy required extra computational work, i.e., θ and its energy dependence had to be treated as independent fit parameters during the analysis. This was performed only once for the clean surface, and the result was used for the subsequent analysis of the $c(2\times2)$-covered phase.

The intensity analysis was performed using the Barbieri/Van Hove symmetrized automated tensor LEED package,[18] in which the perturbation method tensor LEED[19] is combined with an R factor directed automated search algorithm.[20] Atomic scattering was described by relativistically calculated phase shifts which were corrected for thermal vibrations. These were considered by independent variation of the Debye temperatures of the first two substrate layers and using the bulk value (430 K) for deeper layers. Hydrogen was assumed to vibrate with the same amplitude as top substrate layer atoms which is equivalent to Debye temperatures of about 2500 K. For the nominally clean surface the data were calculated up to 400 eV requiring a total of 11 phase shifts, for the analysis of the hydrogen-covered phase 10 phase shifts proved to be sufficient up to 300 eV. The use of renormalized forward scattering (RFS)[21] in the mentioned program package required to treat the close spaced pairs of layers in the (1010) surface (see Fig. 1) as composite layers. Special care was taken not to leave the validity range of tensor LEED during the search procedure. Whenever the algorithm found a structure with one or more atoms having moved away from the reference position(s) by more than 0.02 Å (Re atoms) or 0.05 Å (H atoms), a new reference calculation at the new position(s) was performed. In this way, errors due to the tensor LEED approximation are largely avoided. For the quantitative comparison of experimental and calculated data and for directing the search, again the Pendry R factor R_P (Ref. 22) was used.

B. Hydrogen adsorption on Ru(10$\bar{1}$0)

The LEED experiments for this adsorption system were conducted in an ultrahigh vacuum chamber with a base pressure 1×10^{-10} mbar and equipped with four-grid LEED optics, a cylindrical mirror analyzer for Auger electron spectroscopy (AES), and the usual facilities for surface cleaning and characterization, as described in more detail elsewhere.[23] The sample was cleaned by argon ion bombardment at 1 keV followed by cycles of oxygen adsorption and thermal desorption in order to remove surface carbon, the main contaminant at the surface. Final traces of oxygen were removed by flashing the surface to 1530 K, resulting in a sharp (1×1) LEED pattern. The $c(2\times2)$-3H phase was prepared by exposing the clean surface to 1.1 L hydrogen at 110 K. Using a video-LEED system,[17] intensity spectra were recorded at a sample

temperature of 110 K and at normal incidence of the primary electron beam for both the clean and adsorbate-covered surface.

For the clean surface it turned out that the LEED IV curves changed substantially within a few minutes which is of the order of the data acquisition time. As AES measurements indicate a clean surface, we conclude that the change of LEED intensity is very likely due to adsorption of hydrogen which is inevitably present in the residual gas. Therefore we recorded an additional set of data at 430 K, a temperature where hydrogen is not adsorbed anymore at the surface. The LEED IV curves of the $c(2\times2)$-3H phases turned out to be largely unaffected by residual gas contamination. They were taken for two fractional and five integral-order beams. The resulting cumulative data bases were 2165 eV for the clean surface and 1050 eV for the hydrogen-covered $c(2\times2)$-3H phase.

For the full-dynamical analysis of the LEED data a program developed by Moritz[24] was applied. Besides standard computational schemes for the calculation of intensities it uses a least-squares optimization scheme[25] in order to perform the simultaneous and automated refinement of structural (and nonstructural) parameters. The degree of agreement between calculated and experimental data was quantified by the Pendry reliability factor R_P (Ref. 22) which was also the functional to be minimized in the optimization scheme. The scattering from Ru and H atoms was treated by using up to nine phase shifts which were corrected for thermal vibrations, employing Debye temperatures of 420 K for Ru and 950 K for H held constant during the analysis. The phase shifts have been successfully used in previous LEED analyses of $O/Ru(0001)$,[26] $H/Ni(110)$,[27] and $H/Pd(110)$.[28] The intensity analysis was carried out in two steps. First, an exhaustive grid search over a wide range in parameter space was conducted for the $c(2\times2)$-3H phase with the unrelaxed substrate and the hydrogen atoms located in various positions (see below). In the next step, starting from the optimum parameter values found by the grid searches, automated structure refinements were carried out. Apart from the first three layer spacings, lateral and vertical displacements of Ru atoms in the first, second, and third layer as well as of H atoms (preserving the corresponding local symmetry of the adsorbate) were refined.

The density functional theory calculations are similar to those of the related work of oxygen on Ru(1010).[29] For completeness we repeat the main details. We employed the generalized gradient approximation (GGA) of Perdew *et al.*[30] for the exchange correlation functional. The action of core electrons of ruthenium on valence electrons is replaced by a norm-conserving, fully relativistic pseudopotential using the scheme of Troullier and Martins[31] with core radii $r_c^{l=0.2}=2.48$ bohr and $r_c^{l=1}=2.78$ bohr, and the s component was used as the local component in the Kleinman–Bylander fully separable construction.[32] For hydrogen the plain $1/r$ potential was used. In the $c(2\times2)$ cell we were not able to employ the same k-point sampling as in the earlier calculations, so we did the calculations for both a clean and a hydrogen covered surface using 12 Monkhorst–Pack points[33] in the irreducible Brillouin zone (IBZ) of the $c(2\times2)$ cell, equivalent to 24 points in the IBZ of the (1×1) cell. To stabilize the Brillouin zone integration, the occupation numbers were broadened using a Fermi function with a width of 0.1 eV; the total energies were extrapolated to the case of no broadening. The surface was modeled using the supercell approach with eight layers of Ru(1010) and placing hydrogen on one side of the slab. The calculation scheme allows for the automated relaxation of electrons and atoms, where we relaxed the positions of the H atoms and the atoms in the top two Ru layers, keeping the lower five Ru layer spacings fixed at the bulk values.

III. RESULTS FOR THE ''CLEAN'' SURFACES

As evident from Fig. 1, two terminations are possible for an hcp(1010) surface due to its double layer structure. As both the Re and Ru crystals have similar lattice parameters [a(Re)=2.775 Å, a(Ru)=2.695 Å, c(Re)=4.449 Å, c(Ru)=4.274 Å[34]], the interlayer surface corrugations characteristic of the two terminations also resemble each other. This is about 0.8 Å for the termination by a double layer (termination ''A'' in Fig. 1) and about 1.6 Å for the termination by half a double layer (termination ''B'' in Fig. 1). From earlier work on Re(1010),[35] Co(1010),[36] and Be(1010)[37] we anticipated that only the double layer termination with the smaller corrugation will be stable. Since for Ti(1010) the simultaneous presence of both terminations was reported,[38] we tested both terminations for Ru and Re.

A. Clean Re($10\bar{1}0$)

As already mentioned, the precise angle of incidence and its possible energy dependence $\theta(E)$ are *a priori* not known from experiment. Consequently, we had to determine $\theta(E)$ within the course of the structure determination, a procedure we applied only to the clean surface and whose results were then used for the hydrogen-covered phase. As the LEED data were taken at low temperatures, the surface was presumably slightly hydrogen contaminated. Therefore, the analysis of the data is only meant to retrieve the surface termination and the dependence $\theta(E)$.

Focusing first on the double layer termination, we performed a coarse determination of the angle of incidence. As the experimental estimation is $\theta_0\approx3.4°$, in a first step, the angle was held constant but then varied around this value in steps of 0.2°. The variation of the first two interlayer distances and of the surface Debye temperatures produced a best-fit R factor $R_P=0.24$ for $\theta_0=2.2°$ and the topmost Ru layer spacing contracted by 5%, while the second spacing turned out to be already bulklike (bulk values: $d_{12}=0.797$ Å, $d_{23}=1.593$ Å). This small value for contraction is indicative of some hydrogen contamination. When applying the same analysis to the half double layer termination, an R factor of only $R_P=0.63$ was achieved. This rules out the presence of domains with that termination, as suggested in earlier work for Co(1010).[36]

Eventually, we introduced an energy dependence of both V_{0r} and θ, taking advantage of the large data base which allowed us to fit the two parameters in steps of subsequent energy intervals of 50 eV. The found values fit well to V_{0r}

being proportional to $1/\sqrt{E}$ as also obtained in analyses of other surfaces (see, e.g., Ref. 39). The angle of incidence finally decreases linearly with energy for $E<200$ eV and approaches the constant value $\theta=2.2°$ for $E>200$ eV. In the considered energy range (50–400 eV), this dependence comes close to a $1/\sqrt{E}$, consistent with the presence of some residual magnetic field. By introducing the energy dependences of V_{0r} and θ, the minimum R factor is further reduced to $R_P=0.20$, without affecting the best-fit structural parameters.

B. Clean Ru($10\bar{1}0$)

As expected, the analysis of data taken at 110 K showed (cf. Sec. II A) that the surface is somewhat affected by residual gas adsorption. This is concluded from the result of an almost unrelaxed surface which is in clear contrast to the substantial contraction found for the first layer spacing of Re and Co in earlier investigations.[35,36] Yet, the double layer termination was clearly favored ($R_P=0.25$). The termination by half a double layer produced a very poor agreement between theory and experiment ($R_P=0.67$), so that a coexistence of both terminations can also be ruled out. The LEED data set taken at 430 K (without residual gas contamination) improved the best fit for the double layer termination to the level of $R_P=0.18$, yielding a relaxation of the first and second layer spacings by $10\pm1.5\%$ and $+2.5\pm2.5\%$, respectively (bulk spacings: $d_{12}=1.562$ Å, $d_{23}=781$ Å). These values are in reasonable agreement with previous results found for Re,[35] Co,[36] and Be.[37]

In the DFT calculations, the clean Ru surface was modeled using an eight-layer slab, and the two first substrate layers were relaxed. As expected (due to higher coordination of surface atoms and smaller surface corrugation), the short termination is energetically favored by 41 meV/Å^2 over the long-terminated surface. The surface energy of the short termination is calculated as 176 meV/Å^2 which is $\approx15\%$ larger than our DFT-GGA surface energy for the Ru(0001) surface (154 meV/Å^2). The relaxations of the first and second layer turned out to be $d_{12}/d_0=-13.7\%$ and $d_{23}/d_0=-0.7\%$, thus, a slightly larger inward relaxation is obtained than from the LEED intensity data ($d_{12}/d_0\approx-10\%$).

IV. RESULTS FOR THE HYDROGEN-ADSORBED PHASES

The hcp($10\bar{1}0$) surface offers several high-symmetry sites for hydrogen atoms to reside in. Since for both Re($10\bar{1}0$) and Ru($10\bar{1}0$) the LEED IV curves of integral-order spots do not change very much upon H adsorption, we expect that the surface termination remains unchanged. Considering threefold and also twofold coordinated sites for hydrogen, we are left with six plausible and essentially different models having three H atoms in the $c(2\times2)$ unit cell (H coverage of 3/2). These models are illustrated in Fig. 2 where two further models were added. In model No. 7 the occupation of on-top sites is allowed because this configuration maximizes the lateral distances between H atoms. In model No. 8 ''half'' adatoms, i.e., scatterers of half the hydrogen scattering strength, are introduced. This model can be envisioned as a variant of either model No. 1 with strongly vibrating bridge atoms or model No. 2 with hydrogen atoms statistically sitting on one or the other flank of the densely packed rows. Each of the eight models was thoroughly tested in the course of the analyses.

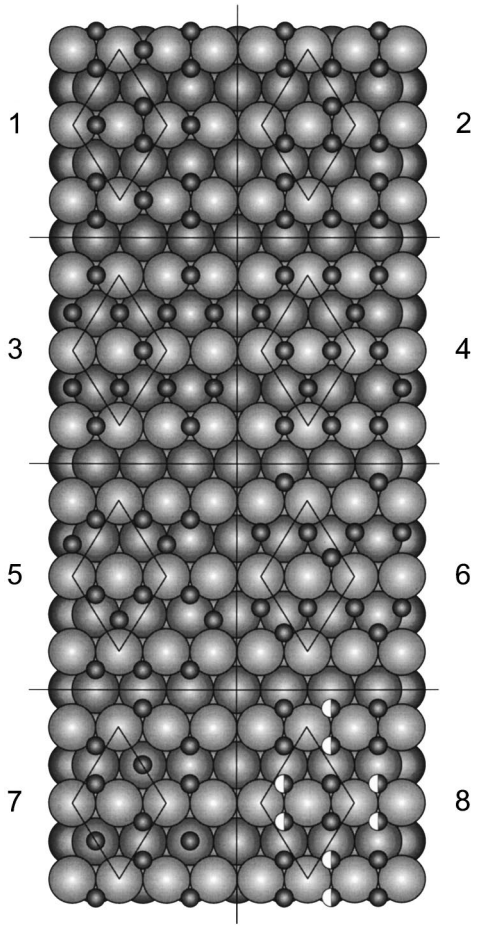

FIG. 2. Structural models tested to retrieve the $c(2\times2)$-3H structure on the (1010) surfaces of Ru and Re.

Moreover, the analyses had to account for the experimental observation that for both the Re and Ru substrates the superstructure spot intensities were on a quite high level, i.e., about 5%–10% of the integral-order beam intensities on the energy average. This cannot originate from mere hydrogen scattering but rather points towards some substrate reconstructions. Evidence of H-induced reconstructions is also provided by the fact that the superstructure beams are visible even at higher energies where the hydrogen scattering becomes practically negligible. Although the reconstruction must be relatively weak according to the still low level of superstructure spot intensities, there is no way to fit the data quantitatively without introducing H-induced displacements of the substrate atoms. Preliminary LEED calculations for the Re($10\bar{1}0$) surface in which hydrogen scattering was completely neglected indicated already that a substantial contribution of the substrate to the intensities of half-order spots comes from a vertical buckling in the third substrate layer. Though this buckling, by symmetry arguments, is compatible only with models No. 1, No. 2, No. 3, No. 6, and No. 8, we

considered it also for the other models. Displacements of atoms in the first two layers, both in-plane and vertical to the layer, were also allowed in the analyses. Since the integral-order spot intensities are only little affected by the weakly scattering hydrogen and by the slight substrate reconstruction, the main source of information about the $c(2\times2)$-3H phase is related to the half-order spot intensities.

A. The phase Re(10$\bar{1}$0)-$c(2\times2)$-3H

The same energy-dependent angle of incidence and inner potential as determined for the clean surface were used for the $c(2\times2)$-3H phase, allowing only an additional constant shift for the inner potential. As starting reference structures for the different models we used the bulklike terminated substrate (double layer termination) with hydrogen at ideal high symmetry positions and hard-sphere radii of $r_{\mathrm{Re}}=1.38$ Å and $r_{\mathrm{H}}=0.53$ Å. During the search any variation of the hydrogen coordinates was allowed as long as the symmetry of the adsorption site was preserved. This means that H atoms in on-top or bridge positions were allowed to shift only vertically, while atoms in quasi-threefold sites could move within a plane normal to the densely packed Re rows. Furthermore, the positions of Re atoms in the first three layers were optimized as far as those were supported by the respective adsorption models. For instance, no first layer buckling was tried for model No. 1, while a lateral pairing along the densely packed rows was considered.

The best-fit Pendry R factors achieved for the subset of half-order spots are $R=0.35$, 0.66, 0.49, 0.89, 0.72, 0.63, 0.76, and 0.43 for the eight investigated models (in the sequence displayed in Fig. 2). Obviously, this favors model No. 1. The variance of the R factor amounts to $\mathrm{var}(R_P)=0.08$, i.e., all models with $R>0.43$ can be ruled out. The all-beam R factors are $R_P=0.30$, 0.37, 0.35, 0.44, 0.39, 0.38, 0.41, and 0.32. The variance of the latter is, due to the large data base, as small as $\mathrm{var}(R_P)=0.04$, so that model No. 1 is also favored on the basis of the *overall* R factor. The only model that is close to the best-fit model No. 1 concerning the R factor is model No. 8. However, this model is simply a variant of model No. 1: All atomic positions are the same within the error limits except the positions of the two ''half'' hydrogen atoms. Although in the starting configuration the hydrogen atoms were placed in the threefold coordinated sites, the fit procedure led to a separation of the ''half'' atoms by 0.48 Å with the same height as for the bridge atom in model No. 1. This may be interpreted as due to thermal vibrations of the bridge bonded atoms simulated by ''split positions''.[40] Altogether (although at a relatively high R-factor level), we can identify the structure of Re(10$\bar{1}$0)-c(2×2)-3H to be that of model No. 1 in Fig. 2. A more detailed picture of the best-fit structure is displayed in Fig. 3, which also defines the structural parameters to be refined. The numerical values determined are compiled in Table I. Experimental and best-fit spectra are displayed in Fig. 4 for a selection of beams.

The best-fit structure found can be described as follows. Two out of three hydrogen atoms in the $c(2\times2)$ unit cell adsorb on quasi-threefold coordinated sites at the flank of the densely packed rows of the substrate in the first layer, attaching two Re atoms in the topmost layer and one in the second layer. The bond length to first layer Re atoms is 1.85 ±0.40 Å, that to the second layer Re atoms is 2.02 ±0.50 Å. This corresponds to hydrogen radii of 0.47 and 0.64 Å, respectively. The third H atom occupies the remaining first layer bridge sites with a H–Re bond length of 1.92 ±0.20 Å, yielding a hydrogen radius of 0.54 Å. The hydrogen radii retrieved here (although with large error bars) match well within the range of values found in the literature (about 0.4–0.7 Å[3,5,13]). The first layer rhenium atoms are shifted pairwise towards the bridge hydrogen position by 0.02 Å, whose value, however, falls within the limits of the statistical errors as derived from the variance of the R factor. The interlayer distances in the substrate d_{12} and d_{23} (as defined with respect to the center of mass plane for buckled layers) are practically bulklike, i.e., the layer relaxation found for the clean surface is lifted by the adsorption of hydrogen as frequently observed for other hydrogen adsorption systems.[5,13] On the other hand, we find the next layer spacing d_{34} contracted by 0.05 Å. Such a contraction can be

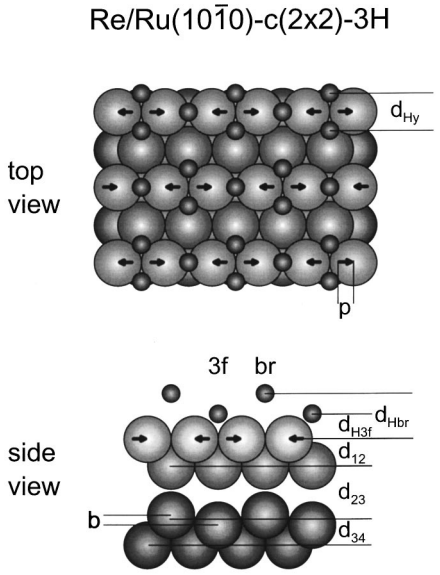

FIG. 3. Top and side view of the resulting best-fit structures being almost identical for Re(10$\bar{1}$0)-$c(2\times2)$-3H and Ru(10$\bar{1}$0)-$c(2\times2)$-3H. In order to visualize the important features of the structure, buckling and layer distances do not scale but are exaggerated.

TABLE I. Numerical values of the best-fit model parameters as defined in Fig. 3 [bulk values for interlayer spacings of Re (Ru) are $d_{12}=d_{34}=0.797(0.78)$ Å and $d_{23}=1.593(1.56)$ Å].

Method	LEED	LEED	DFT
substrate	Re	Ru	Ru
d_{Hy} (Å)	1.88	2.23	2.18
$d_{\mathrm{H3}f}$ (Å)	0.76	0.97	0.77
$d_{\mathrm{H}br}$ (Å)	1.36	1.4	1.23
p (Å)	0.02	0.02	0.03
b (Å)	0.06	0.06	0.00
d_{12} (Å)	0.79	0.83	0.80
d_{23} (Å)	1.6	1.55	1.59
d_{34} (Å)	0.74	0.69	0.80

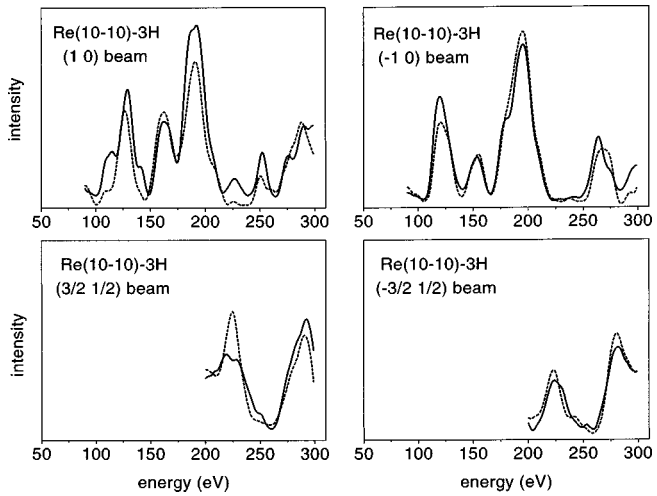

FIG. 4. Selected best-fit spectra of Re(10$\bar{1}$0)-$c(2\times2)$-3H. The R factor averaged over all beams is 0.30 (0.28 and 0.35 for integral and half-order beams, respectively). Solid and dashed lines represent experimental and theoretical data, respectively.

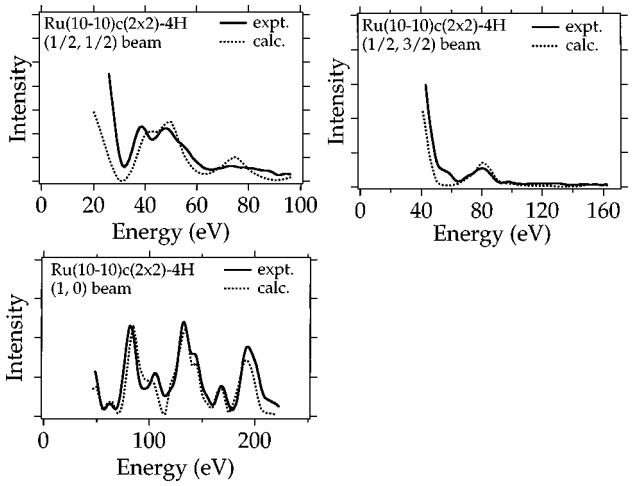

FIG. 5. Selected best-fit spectra of Ru(10$\bar{1}$0)-$c(2\times2)$-3H. The R factor averaged over all beams is 0.23 (0.20 and 0.30 for integral and half-order beams, respectively). Solid and dashed lines represent experimental and theoretical data, respectively.

excluded for the clean surface, as was checked by additional test calculations. The contraction is accompanied by a relatively strong buckling of 0.06 Å in the third layer which, however, is just at the boarder of the error limits. As compared to the clean surface, it seems that H atoms adsorbed in threefold sites push adjacent Re atoms in the third layer inwards, while H atoms in bridge sites do not alter the positions of the respective third layer Re atoms.

B. The phase Ru(10$\bar{1}$0)-$c(2\times2)$-3H

The search strategy which had been proven successful for the Re(10$\bar{1}$0)-$c(2\times2)$-3H surface was also adopted for Ru(10$\bar{1}$0)-$c(2\times2)$-3H. In the analysis we considered only the fractional-order beams and one integral-order beam in order to enhance the sensitivity of the analysis (cf. discussion of the Re(10$\bar{1}$0)-$c(2\times2)$-3H phase) with respect to the structure parameters related to the $c(2\times2)$ unit cell. The optimum R factors for this subset of beams were 0.30, 0.42, 0.36, 0.47, 0.55, 0.38, 0.51, and 0.35 for the models given in Fig. 2. Again model No. 1 is favored. The numerical values of the best-fit structural parameters defined in Fig. 3 are summarized in Table I; the experimental versus best-fit LEED IV curves are displayed in Fig. 5 for a selection of beams. The best-fit structure found is very similar to that of the Re case. The bond length of the quasi-threefold coordinated H atom to first layer ruthenium atoms is 2.01 ± 0.40 Å, while that to the second layer ruthenium atoms amounts to 2.06 ± 0.50 Å. This corresponds to hydrogen radii of 0.65 and 0.70 Å, respectively. The third H atom again occupies remaining first-layer bridge sites with a H–Ru bond length of 1.95 ± 0.20 Å which corresponds to a hydrogen radius of 0.60 Å. The adsorbate-induced displacements of substrate atoms are virtually identical to those found for the H/Re phase, i.e., first layer substrate atoms are shifted pairwise towards the bridge hydrogen position by 0.02 Å, and there is a relatively strong buckling of 0.06 Å in the third layer. The interlayer distances d_{12} and d_{23} are practically bulklike, while, again similar to H/Re, the spacing d_{34} is contracted (by 0.09 Å). Except for the effective hydrogen radii, which for threefold coordinated sites on Ru are smaller than on Re, the results for H/Re and H/Ru are virtually identical, lending further support to the unusual bridge adsorption site of H.

DFT-GGA calculations were performed only for the structure model No. 1 to save computer time. The structural parameters are summarized in Table I together with the LEED results. The agreement is considered very good, especially regarding the error bars of experiments and that the nucleus of hydrogen, a proton, was treated as pointlike in the DFT calculations, i.e., the zero point vibrations were not included. The third layer was not allowed to relax and, thus, the magnitude of the buckling is not available. However, the forces parallel to the surface normal on the two atoms in the third layer were in opposite direction, thus supporting the LEED geometry.

In order to elucidate the change of work function with increasing hydrogen coverage,[3] we performed further DFT calculations for the coverages one and two in a 1×1 cell. The (1×1)-2H (hcp-hcp) phase has been observed experimentally in contrast to the (1×1)-H phase which was studied by DFT to extract information on the bonding and site preference at lower coverages. The results are compiled in Table II: For the case of one H atom per (1×1) unit cell, hydrogen atoms prefer adsorption in twofold coordinated sites. The same configuration was reached on relaxing the electronic system and the atomic coordinates even when the hydrogen atom was initially positioned at the hcp site obtained from the (1×1)-2H structure. The results in Table II and the charge density differences (cf. Fig. 6) explain the trend in work function: Hydrogen, a more electronegative element than ruthenium, acts as an acceptor and therefore increases the work functions. For Ru(10$\bar{1}$0) the highest value of the work function at about coverage one is most likely related to hydrogen atoms sitting in (quasi-) bridge sites. At coverage two both of the hydrogen atoms reside in hcp sites exhibiting a smaller dipole moment and, although the num-

TABLE II. Hydrogen coverage Θ, coordination s, adsorption energy E_{ads}, work function change $\Delta\Phi$, and H-Ru distances in different overlayer structures of Ru(1010) [and Ru(0001): last row]. The adsorption energy is calculated with respect to a hydrogen atom in gas phase. Ru(1) denotes the outermost layer Ru atoms and Ru(2) the second layer atoms. In the $c(2\times2)$-3H structure, the distances of hydrogen atoms to Ru(1) and Ru(2) at both sites (hcp and short bridge) are indicated. The energies are in electron volts and the distances in angstroms. The experimental values of $\Delta\Phi$ for H-Ru(1010) are 0.42, 0.36, and 0.25 eV for H coverages of 1.0, 1.5, and 2.0, respectively (Ref. 3).

Structure	Θ	s	E_{ads}	$\Delta\phi$	$z_{\text{H-Ru(1)}}$	$d_{\text{H-Ru(1)}}$	$d_{\text{H-Ru(2)}}$	$d_{\text{H}_{br}\text{-Ru(1)}}$
(1×1)-H	1	2	2.79	0.79	1.04	1.85	2.39	
$c(2\times2)$-3H	3/2	3+3+2	2.73	0.64	1.23+0.77	1.95	1.92	1.83
(1×1)-2H(hcp-hcp)	2	3+3	2.71	0.36	0.76	1.91	1.94	
Ru(0001)-(1×1)-1H	1	3	2.86	0.08	1.02	1.91		

ber of atoms in the cell increases, the work function is lower than at coverage 3/2. The fact that the change in work function at Ru(0001) is much smaller, although the height of the hydrogen atom above the surface is similar, suggests the hydrogen atom to be more negative on Ru(1010) than on Ru(0001).

V. DISCUSSION AND CONCLUSION

There do not exist very many structural analyses of H superstructures on anisotropic row-and-trough surfaces such as fcc(110), bcc(211), or hcp(1010).[2,13] With Ru being a platinum group metal, it is tempting to compare its hydrogen adsorptive behavior with Ni or better its 4*d* congeners Rh or Pd. On none of these surfaces hydrogen orders into a $c(2\times2)$ lattice, rather zigzag or linear chains with (2×1) and/or (1×2) periodicity are formed. While a strong pairing-row reconstruction occurs on Ni(110)[27] and Pd(110),[28] there is a less pronounced (1×2) buckling reconstruction found for Rh(110).[41] In all these cases, no evidence of bridge site occupation was found.[27,28,41] These findings are supported by vibrational loss measurements: As demonstrated for the pairing-row reconstruction Ni(110)-(1×2)-3H phase by applying selection rules for both dipole and impact electron scattering,[42] there is such a high tendency of the H atoms to choose a site with threefold coordination that the hydrogen atoms even refuse available (quasi-) fourfold sites and prefer to reside in threefold sites. For H adsorption on the Rh(110) surface, vibrational loss measurements revealed that the H atoms adsorb in the quasi-threefold coordinated sites provided by the (111) microfacets on the Rh(110) surface,[43] in agreement with the LEED results.[41]

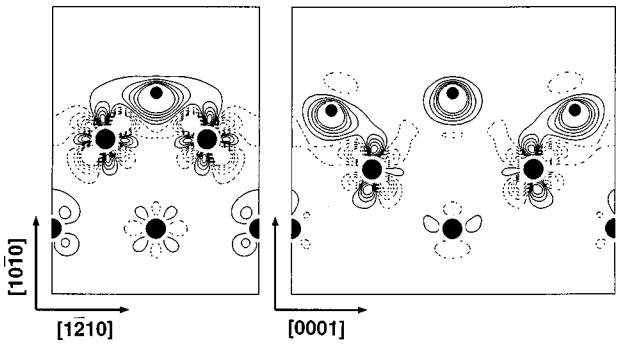

FIG. 6. Change in the electron density due to hydrogen chemisorption on Ru(10$\bar{1}$0) [Ru(1010)-$c(2\times2)$-3H surface] with respect to the clean Ru(1010) surface and an unsupported H overlayer. Large filled circles are Ru atoms, and small filled circles represent the hydrogen atoms. Left side: A cut of the difference electron density along the densely packed Ru rows in the [1210] direction intersecting the hydrogen atom in the short bridge site (cf. Fig. 3). Right side: A cut of the difference electron density map perpendicular to the densely packed rows crossing the hydrogen atoms in hcp sites and the bridge site (cf. Fig. 3). Solid lines indicates electron accumulation while the dashed line indicates electron depletion. Clearly, the hydrogen atoms act as electron acceptors in the Ru(10$\bar{1}$0)-$c(2\times2)$-3H system. The Ru–H bonding appears covalent.

Previous and more recent HREELS measurements performed with both H/Ru(1010)[14,44] and H/Re(1010)[45] may provide further clues on the local symmetry of the H adsorption site. Unfortunately, the evidence of all available HREELS results is not too revealing due to low cross sections for dipole as well as for impact excitations of the H surface vibrations. The loss intensities, especially for the Re surface, are rather low, and for none of the observed vibrational bands is there a clear-cut identification of a C_{2v} symmetry (which one would expect for H atoms adsorbed in bridge positions). There is still another puzzling feature concerning the cross section for vibrational excitation. A hydrogen atom which resides in a bridge position on top of a Ru (Re) row sticks out considerably. For such a situation a rather strong excitation by the low-energy electron wave in the HREELS experiment was found for H/W(100),[9] and consequently, an intense loss feature was observed. This, however, is not encountered in the present case where just those vibrations which appear along with the $c(2\times2)$ structure at coverage $\theta=3/2$ are particularly weak. Yet, the cross section for the energy-loss process might depend on the details of the electronic properties of the surface.

Nevertheless, the LEED and DFT data presented here are internally consistent, and the reliability factors are satisfactory. From the eight different surface geometries chosen (Fig. 2) model No. 1 in each case comes closest to experiment, while model No. 5 (which has been previously proposed[16]) yields a much worse *R* factor, in particular for half-order spots. With this high probability of model No. 1 being the real surface structure, we have shown that (i) the influence of H atoms on rather corrugated surfaces [such as hcp(1010) planes] can lead to even third layer buckling effects, and (ii) H atoms can occupy bridge sites, which underlines that the high melting point metals Ru and Re rather

resemble the refractory metals molybdenum and tungsten, where H atoms were reported to occupy bridge sites.[8–12] One reason why apparently a site with reduced coordination is chosen seems to be the competition between the local energy gain (which calls for the occupation of a highly coordinated site) and the mutual H–H interactions (which favor an overall homogeneous distribution of the H atoms within the adsorbed layer). Our results suggest that [at least for the $c(2\times2)$ phase with coverage 3/2] a nearly homogeneous distribution of H atoms, with a maximum of high coordination sites occupied, represents the most favorable situation.

An alternative explanation why the bridge site is occupied by hydrogen could emerge by comparing our results with those of recent LEED calculations for H/Be(0001)[46] and DFT calculations of H/Al(111).[47] On both surfaces hydrogen adsorption is predicted to proceed in bridge sites. The driving force to occupy bridge sites is even so strong that both close-packed surfaces undergo a reconstruction into a $(\sqrt{3}\times\sqrt{3})R30°$ vacancy structure, as it has been identified for K adsorption on Al(111)[48] and which is related to the particular sp^2 hybridization at the substrate surface. It may be that the s-p charge density at Ru(10$\bar{1}$0) and Re(10$\bar{1}$0) (in for low-coordinated substrate atoms) plays an equally important role as on Al(111) and Be(0001). Of course we are aware of the fact that Re and Ru are typical candidates of d metals rather than of s-p metals. However, the bonding state of hydrogen is about 5 to 6 eV below the Fermi level and there the s-p charge density dominates the total (energy resolved) charge density.

To elucidate the electronic reasons behind the bridge site occupation, detailed *ab initio* calculations are required. Preliminary DFT calculations for the H–Ru(1010) system with a (1×1) unit cell indicated that the energy difference between bridge sites and threefold hcp sites is actually very small, i.e., of the order of several 10 meV, so that bridge site occupation is not that disfavorable, as one might expect at first glance (cf. Table II). As a consequence, the delicate energy balance may be governed by a minimization of the mutual H–H repulsion which may, in turn, determine the actual arrangement of the hydrogen atoms. Using structure model No. 1, as predicted here by LEED, total energy calculations were performed for the Ru(1010)-$c(2\times2)$-3H phase in order to determine the structural parameters (the values are collected in Table I, right column). The DFT results are in good agreement with the LEED results. The sensitivity of DFT calculations to the hydrogen position may be considered higher than that of LEED, and therefore the H positions provided by DFT (which differ from the LEED predictions) can be regarded as more reliable. The effective radius of threefold coordinated hydrogen is about 0.6 Å and that of bridge bonded hydrogen 0.5 Å. Both values agree quite nicely with values found on Re(10$\bar{1}$0). The experimentally observed maxima in the work function changes of the H-Ru(1010) system as a function of the H coverage can be traced back to hydrogen atom occupying bridge sites. On Ru(1010) chemisorbed hydrogen atoms act as an electron acceptor.

In summary, our LEED analyses (in combination with the DFT calculations) of the $c(2\times2)$-3H phases on the (10$\bar{1}$0) surfaces of both Re and Ru below 200 K and at a hydrogen coverage of 3/2 yield rather surprising features: Both threefold and bridge sites are occupied by the H atoms, and reconstruction effects are apparently restricted to a third layer buckling, along with a slight displacement of those substrate row atoms which are ''clamped together'' by a bridging H atom.

ACKNOWLEDGMENT

The authors gratefully acknowledge financial support by the Deutsche Forschungsgemeinschaft (DFG).

[1] Z. Knor, in *Catalysis*, edited by J. R. Anderson and M. Boudart (Springer, Berlin, 1982), Vol. 3, p. 231.
[2] K. Christmann, J. Mol. Phys. **66**, 1(1989).
[3] K. Christmann, Surf. Sci. Rep. **9**, 1 (1988).
[4] J. W. Davenport and P. J. Estrup, in *The Chemical Physics of Solid Surfaces and Heterogeneous Catalysis*, edited by D. A. King and D. P. Woodruff (Elsevier, Amsterdam, 1990), Vol. 3A, p. 1.
[5] K. Heinz and L. Hammer, Phys. Status Solidi A **159**, 225 (1997).
[6] K. Heinz and L. Hammer, Z. Phys. Chem. (Munich) **197**, 173 (1996).
[7] K. H. Rieder, Surf. Rev. Lett. **1**, 51 (1994).
[8] M. A. Passler, B. W. Lee, and A. Ignatiev, Surf. Sci. **150**, 263 (1985).
[9] R. F. Willis, W. Ho, and E. W. Plummer, Surf. Sci. **80**, 593 (1979); R. F. Willis, *ibid.* **89**, 457 (1979).
[10] P. J. Estrup, J. Vac. Sci. Technol. **16**, 635 (1979).
[11] F. Zaera, E. B. Kollin, and J. L. Gland, Surf. Sci. **166**, L149 (1986).
[12] L. Hammer, M. Kottcke, A. Wimmer, D. M. Zehner, and K. Heinz, Surf. Sci. (in press).
[13] NIST Surf. Struct. Database 2.0 (1995), Nat. Inst. Stand. Technol., Gaithersburg.
[14] G. Lauth, E. Schwarz, and K. Christmann, J. Chem. Phys. **91**, 3729 (1989).
[15] U. Muschiol, J. Lenz, E. Schwarz, and K. Christmann, Surf. Sci. **331–333**, 127 (1995).
[16] K. Christmann and U. Muschiol, Z. Phys. Chem. (Munich) **197**, 155 (1997).
[17] P. Heilmann, E. Lang, K. Heinz, and K. Müller, in *Determination of Surface Structure by LEED*, edited by P. M. Marcus and F. Jona (Plenum, New York, 1984), p. 463; K. Heinz, Prog. Surf. Sci. **27**, 239 (1988).
[18] Barbieri/Van Hove, Symmetrized Automated Tensor LEED package, available from M. A. Van Hove.
[19] P. J. Rous, J. B. Pendry, D. K. Saldin, K. Heinz, K. Müller, and N. Bickel, Phys. Rev. Lett. **57**, 2951 (1986); P. J. Rous and J. B. Pendry, Surf. Sci. **219**, 355 (1989); Surf. Sci. **219**, 373 (1989); P. J. Rous, Prog. Surf. Sci. **39**, 3 (1992).
[20] P. J. Rous, M. A. Van Hove, and G. A. Somorjai, Surf. Sci. **226**, 115 (1990); M. A. Van Hove, W. Moritz, H. Over, P. J. Rous, A. Wander, A. Barbieri, N. Materer, U. Starke, D. Jentz, J. M. Powers, G. Held, and G. A. Somorjai, *ibid.* **287**, 431 (1993).
[21] J. B. Pendry, *Low Energy Electron Diffraction* (Academic, London, 1974).
[22] J. B. Pendry, J. Phys. C **13**, 937 (1980).
[23] H. Over, H. Bludau, M. Skottke-Klein, G. Ertl, W. Moritz, and C. T. Campbell, Phys. Rev. B **45**, 8638 (1992).
[24] W. Moritz, J. Phys. C **17**, 353 (1983).
[25] G. Kleinle, W. Moritz, and G. Ertl, Surf. Sci. **238**, 119 (1990); H. Over, U. Ketterl, W. Moritz, and G. Ertl, Phys. Rev. B **46**, 15438 (1992); M. Gierer, H. Over, and W. Moritz (unpublished).
[26] C. Stampfl, S. Schwegmann, H. Over, M. Scheffler, and G. Ertl, Phys. Rev. Lett. **77**, 3371 (1996).
[27] G. Kleinle, V. Penka, R. J. Behm, G. Ertl, and W. Moritz, Phys. Rev. Lett. **58**, 148 (1987).
[28] M. Skottke, R. J. Behm, G. Ertl, V. Penka, and W. Moritz, J. Chem. Phys. **87**, 6191 (1987).
[29] S. Schwegmann, A. P. Seitsonen, V. De Renzi, H. Dietrich, H. Bludau, M. Gierer, H. Over, K. Jacobi, M. Scheffler, and G. Ertl, Phys. Rev. B (in press).
[30] J. P. Perdew, J. A. Chevary, S. H. Vosko, K. A. Jackson, M. R. Pederson, D. J. Singh, and C. Fiolhais, Phys. Rev. B **46**, 6671 (1992).
[31] N. Troullier and J. L. Martins, Phys. Rev. B **43**, 1991 (1993).

[32] L. Kleinman and D. M. Bylander, Phys. Rev. Lett. **48**, 1425 (1982).
[33] H. J. Monkhorst and J. D. Pack, Phys. Rev. B **13**, 5188 (1976).
[34] D'Ans-Lax, *Taschenbuch für Chemiker und Physiker* (Springer, Berlin, 1967).
[35] H. L. Davis and D. M. Zehner, J. Vac. Sci. Technol. **17**, 190 (1980).
[36] H. Over, G. Kleinle, W. Moritz, G. Ertl, K.-H. Ernst, H. Wohlgemuth, K. Christmann, and E. Schwarz, Surf. Sci. **254**, L469 (1991).
[37] Ph. Hofmann, K. Pohl, R. Stumpf, and E. W. Plummer, Phys. Rev. B **53**, 13715 (1996).
[38] P. R. Watson and J. Mischenko III, Phys. Rev. B **42**, 3415 (1990).
[39] W. Hösler, W. Moritz, E. Tamura, and R. Feder, Surf. Sci. **171**, 55 (1986).
[40] H. Over, W. Moritz, and G. Ertl, Phys. Rev. Lett. **70**, 315 (1993); H. Over, M. Gierer, H. Bludau, and G. Ertl, Phys. Rev. B **52**, 16812 (1995).
[41] W. Puchta, W. Nichtl, W. Oed, N. Bickel, K. Heinz, and K. Müller, Phys. Rev. B **39**, 1020 (1989); W. Nichtl-Pecher, W. Oed, H. Landskron, K. Heinz, and K. Müller, Vacuum **41**, 297 (1990); K. Heinz, W. Nichtl-Pecher, W. Oed, H. Landskron, M. Michl, and K. Müller, Springer Series in Surface Science **24**, 401 (1991).
[42] B. Voigtländer, S. Lehwald, and H. Ibach, Surf. Sci. **208**, 113 (1989).
[43] H. J. Müssig, W. Stenzel, Y. Song, and H. Conrad, Surf. Sci. **311**, 295 (1994).
[44] M. Gruyters and K. Jacobi, J. Cryst. Growth **64/65**, 591 (1993).
[45] U. Muschiol, Doctoral thesis, Freie Universität Berlin, 1997.
[46] R. Stumpf, Phys. Rev. B **53**, 4253 (1996); K. Pohl, J. B. Hannon, and E. W. Plummer, ECOSS 16, Genoa (Italy) (1996).
[47] R. Stumpf, Phys. Rev. Lett. **78**, 4454 (1997).
[48] C. Stampfl, M. Scheffler, H. Over, J. Burckhardt, M. Nielsen, D. L. Adams, and M. Moritz, Phys. Rev. Lett. **69**, 1532 (1992).